URG11 promotes proliferation and induced apoptosis of LNCaP cells

CHENMIN SUN[1], GUANGMING ZHANG[1], SHUJIE CHENG[2], HAINING QIAN[2], DONG LI[2] and MIN LIU[2]

Departments of [1]Anesthesiology and [2]Urology, Tongren Hospital Shanghai Jiao Tong University School of Medicine, Shanghai 200336, P.R. China

Received October 16, 2018; Accepted February 27, 2019

DOI: 10.3892/ijmm.2019.4121

Abstract. von Willebrand factor C and EGF domain-containing protein (URG11), a cell growth regulator, is involved in the progression of a variety of types of cancer, including prostate cancer (Pca). However, the functions of the URG11 gene in Pca cells require in-depth investigation. The mRNA and protein levels of URG11 were measured by reverse transcription quantitative polymerase chain reaction (RT-qPCR) and western blot analysis. Cell Counting kit-8 (CCK-8), wound-healing and Transwell assays were used to detect cell viability, migration and invasion, respectively. Apoptosis and cell cycle analyses were performed using flow cytometry. The mRNA and protein expression levels of epithelial (E)-cadherin, vimentin, α-smooth muscle actin (α-SMA), cyclin D1 and MYC proto-oncogene protein (c-Myc) were analyzed by RT-qPCR and western blot analysis. In the present study, the mRNA and protein levels of URG11 were markedly upregulated in Pca cell lines compared with those in the normal prostate epithelial cell line. With functional experiments, the cell viability, migration and invasion of Pca cells were markedly promoted by URG11 overexpression. The cell cycle was effectively induced by URG11 and apoptosis was inhibited by the overexpression of URG11. Concomitantly, the epithelial marker E-cadherin was downregulated, and the mesenchymal markers vimentin and α-SMA were upregulated following URG11 overexpression. By contrast, genetic knockout of URG11 elicited the opposite effects. The present study also identified that the downstream effector genes of the Wnt/β-catenin signal pathway, cyclin D1 and c-Myc, were increased following the overexpression of endogenous URG11, which are known to regulate cell proliferation. In addition, the Wnt/β-catenin inhibitor FH535 ameliorated the promotive effects of URG11 on LNCaP cells viability, migration and invasion, and the Wnt/β-catenin agonist LiCl reversed the inhibitory effects of siURG11 in LNCaP cells on cell viability, migration and invasion. The present study demonstrated that URG11 served an oncogenic role in the development of Pca cells and provided evidence that URG11 has potential as a novel therapeutic target in Pca.

Correspondence to: Dr Dong Li or Dr Min Liu, Department of Urology, Tongren Hospital Shanghai Jiao Tong University School of Medicine, 1111 Xianxia Road, Shanghai 200336, P.R. China
E-mail: lidong_dli@163.com
E-mail: lmin_minliu@163.com

Key words: von Willebrand factor C and EGF domain-containing protein, prostate cancer, invasion, migration

Introduction

Prostate cancer (Pca) is a common malignant tumor in men and is also the second most serious malignant tumor that threatens mens' health (1,2). Patients with Pca do not exhibit clear symptoms in the early stages of the disease, resulting in ~20% of patients presenting with metastasis at the time of diagnosis, thereby missing the optimal window for surgical treatment (3,4). Therefore, the identification of novel methods for the early diagnosis of Pca and the corresponding treatments have attracted much attention.

von Willebrand factor C and EGF domain-containing protein (URG11), located on the long arm of human chromosome 1, encodes a 70 kDa protein containing 5 von Willebrand factor type C domains; of these, the primary domain is 1 C-type lectin (5). The function of URG11 is to regulate cell adhesion, migration and interaction, and it is closely associated with signal transduction (6,7). Previous studies have confirmed that URG11 is not only expressed in various tumor cells and tissues including hepatocellular carcinoma (8), and gastric (9) and pancreatic cancer (10), and may promote the occurrence and development of tumors, it is considered to serve as a regulator of cell growth (10,11). In a previous study, URG11 was overexpressed in Pca tissues and detected by immunohistochemistry, and was demonstrated to be positively correlated with Gleason score and clinical stage of Pca, and closely associated with the development of Pca (12). Epithelial-mesenchymal transition (EMT) refers to the process through which epithelial cells gradually lose their epithelial differentiation characteristics and obtain an interstitial phenotype (13). In this process, adhesion between epithelial cells and basement membrane gradually disappears; instead, changes in the cytoskeleton and shape are observed. In addition, an increase in podoplanin and motor abilities, and enhanced migratory and invasive abilities have been identified (14,15). In the process of embryonic development

and the formation of organs, cells may diffuse from the primary tissue through EMT, and migrate to secondary tissue sites to continue to grow and differentiate (16,17). EMT is activated again during wound healing, tissue fibrosis and tumor metastasis (18,19).

Previous studies have indicated that one of the most important pathways in the development of EMT in epithelial cells is the Wnt/β-catenin signaling pathway (20). The activation of Wnt/β-catenin signaling induces motility, invasiveness, cell fate determination and maintenance of self-renewal potential (21). Additionally, it was suggested that Wnt/β-catenin signaling is required for the biological processes of metastasis in Pca (22). In the present study, the corresponding agonists and inhibitors of Wnt/β-catenin signaling were used to explore the role of Wnt/β-catenin signaling in Pca. The results provided a basis for a treatment method for Pca by overexpressing or silencing the regulation of URG11 in Pca cells.

Materials and methods

Reagents. The 293 cell line, human normal prostate epithelial RWPE-1 cell line, and human Pca DU-145, PC-3 and LNCaP cell lines were obtained from the American Type Culture Collection (Manassas, VA, USA). FH55 [F5682; high performance liquid chromatography (HPLC) purity ≥98%] and LiCl (746460; HPLC ≥99%) were purchased from Sigma-Aldrich; Merck KGaA (Darmstadt, Germany).

Cell culture. All cells were placed in RPMI-1640 medium (HyClone; GE Healthcare Life Sciences, Logan, UT, USA), and cultured with 5% CO_2 at 37˚C, under saturated humidity. The cells in logarithmic growth phase were detected.

Cell transfection. Lipofectamine® 3000 (Invitrogen; Thermo Fisher Scientific, Inc., Waltham, MA, USA) was performed following the manufacturer's protocol. In brief, 2 μl Lipofectamine® 3000, 40 pmol small interfering (si) RNA targeting URG11 and the negative control (siNC; Shanghai GenePharma Co., Ltd., Shanghai, China) were mixed separately in 50 μl serum-free medium and incubated at room temperature for 15 min. The lipid compounds were diluted in 300 μl serum-free medium and 600 μl medium containing fetal bovine serum (FBS) to produce a 1 ml volume mixture, and incubated with the LNCaP cells at 37˚C with 5% CO_2. The URG11-targeting siRNA sequence and NC siRNA were 5'-CAGACGGAUUGCUGUACUU-3', and 5'-UUCUCCGAACGUGUCACGUTT-3', respectively. For the expression vectors used to upregulate URG11 (pcDNA3.1-URG11) and the corresponding NC (pcDNA3.1-NC), 5 μl Lipofectamine® 3000 and 2 μg vector (Shanghai GenePharma Co., Ltd.) were mixed in 125 μl Dulbecco's modified Eagle's medium (DMEM; Corning Inc., Corning, NY, USA) and incubated at room temperature for 5 min. A total of 4 μl Lipofectamine® 3000 and 125 μl DMEM were mixed, and incubated at room temperature for 5 min. Then, the Lipofectamine® 3000 + DNA mixture was combined with the Lipofectamine® 3000 + DMEM solution. After 5 min, the LNCaP cells were treated with the combined mixture at 37˚C with 5% CO_2. The cells were transfected for 48 h for subsequent experiments.

Transwell assay detects cell invasion. The LNCaP cells of each treatment group were collected, and $1x10^5$ cells/well were counted. Following the addition of Matrigel (BD Biosciences, Franklin Lakes, NJ, USA) into the Transwell chamber for 6 h at 37˚C, the cells was resuspended in serum-free medium and added to the chamber of the Transwell cell culture plate. Following incubation with 5% CO_2 for 24 h at 37˚C, the chamber was removed, and cells were fixed in 4% paraformaldehyde for 20 min at 4˚C and washed once with PBS. The cells were then stained with 0.1% crystal violet for 10 min at room temperature, washed once with PBS, and observed under a light microscope. Images of the cells were captured and the number of cells that had passed through the membrane was counted in 5 fields using a light microscope at magnification, x200. The number of cells per field was calculated, and experiments were repeated 3 times.

Cell migration assay. LNCaP cells in the logarithmic growth phase (~$1x10^9$ cells/well) were collected, and the suspension was uniformly inoculated into a 6-well culture plate and cultured in an incubator with 5% CO_2 at 37˚C. The control group was cultured in serum-free RMPI-1640 medium, and the experimental group was treated with drug-containing (20 μM FH535 or 20 mM LiCl) serum-free RMPI-1640 medium for 48 h at 37˚C. Following scratching, images of the samples were captured at 0 and 48 h. The scratch healing was observed under an inverted light microscope at magnification, x200. The scratch widths at 8 different sites in the groups were measured by Image-Pro Plus 6.0 software (Media Cybernetics Inc., Rockville, MD, USA) and the cell migration rate in each group was calculated.

Cell Counting kit-8 (CCK-8) assay. A CCK-8 assay (Beyotime Institute of Biotechnology, Haimen, China) was utilized to assess cell viability according to the manufacturer's protocols. Briefly, transfected and un-transfected LNCaP cells were transferred to 96-well plates ($3x10^3$ cells/well). Following incubation for 2 h at 37˚C in 10 μl CCK-8, the absorbance in every well was evaluated using a microplate reader at 450 nm (Tecan Infinite M200 Micro Plate Reader; Tecan Group, Ltd., Männedorf, Switzerland).

Apoptosis assay. Following transfection of the LNCaP cells for 48 h, $1x10^6$ cells were collected, and 1 ml trypsin was used to digest the cells. The mixture was then gently shaken. Following removal of the trypsin and incubation for 1 min at room temperature, the digestion was terminated by adding DMEM containing 10% FBS (Corning Inc.). The cells were centrifuged at 1,000 x g for 3 min at 4˚C and the supernatant was removed. The cells were then washed twice with pre-cooled PBS and resuspended in 1X Annexin V binding buffer. According to the protocol of the manufacturer of the Annexin V-fluorescein isothiocyanate (FITC) cell apoptosis detection kit (K201-100; BioVision, Inc., Milpitas, CA, USA), the cells was stained with 1.25 μl Annexin V-FITC and 10 μl propidium iodide (PI) for 10 min at room temperature, and measured by flow cytometry (FACSCalibur™; BD Biosciences) using FlowJo v10.0 software (FlowJo LLC, Ashland, OR, USA)

Cell cycle analysis. Following transfection for 48 h, $1x10^6$ LNCaP cells/well were collected, washed twice with

PBS, then fixed with 70% ethanol at 4˚C overnight. Then, 500 μl PBS containing 50 mg/l PI, 100 mg/l RNase A and 0.2% Triton X-100 was added to the cells, which were incubated for 30 min at 4˚C in the dark. Flow cytometry was performed, and the results were analyzed using the cell cycle fitting software ModFit LT™ software v2.0 (BD Biosciences).

RNA extraction and reverse transcription quantitative polymerase chain reaction (RT-qPCR). Following culture of the RWPE-1, DU-145, PC-3 and LNCaP cells for 24 h in the medium, the culture solution was discarded and the cells were washed twice with PBS. Then, 500 μl TRIzol (Thermo Fisher Scientific, Inc.) was added to the wells of each 6-well plate, pipetted several times, and then the lysate was transferred to 1.5 ml RNase-free EP tubes. Then, 200 μl chloroform per 1 ml TRIzol was added into the EP tube, and incubated on ice for 10 min. Following centrifugation at 12,000 x g for 15 min at 4˚C, the upper aqueous phase was carefully pipetted into a second RNase-free EP tube; the same volume of isopropanol was the added to the EP tube, and the solution was mixed by inversion several times, and incubated on ice for 10 min. Following centrifugation at 10,000 x g for 5 min at 4˚C, the supernatant was discarded, an equal volume of 75% ethanol was added, and the sediment at the bottom was gently agitated, centrifuged at 7,500 x g for 5 min at 4˚C, and the RNA was air-dried at the vent. Subsequently, 10 μl of DEPC water was added and the RNA concentration and purity were measured using a NanoDrop 2000 spectrophotometer (NanoDrop Technologies; Thermo Fisher Scientific, Inc., Wilmington, DE, USA). A total of 1 μg RNA was used for reverse transcription into cDNA using a reverse transcription cDNA kit (Thermo Fisher Scientific, Waltham, MA, USA). The reaction conditions were as follows: 42˚C for 60 min and 70˚C for 5 min, followed by preservation at 4˚C. SYBR-Green PCR Master Mix (Roche Diagnostics, Basel, Switzerland) was used to conduct the qPCR experiment using an Opticon RT-PCR Detection System (ABI 7500; Thermo Fisher Scientific, Inc.), The PCR thermocycler conditions were as follows: Pretreatment at 95˚C for 10 min; followed by 40 cycles at 94˚C for 15 sec, 60˚C for 1 min and 60˚C for 1 min, and then preservation at 4˚C. The comparative cycle threshold ($2^{-\Delta\Delta Cq}$) method was employed to analyze the expression of mRNA (23). GAPDH expression was used for normalization. The primer sequences used are summarized in Table I.

Western blot analysis. Total proteins were collected by radioimmunoprecipitation assay lysis buffer (Cell Signaling Technology, Inc., Danvers, MA, USA). BCA Protein Assay kit (Pierce; Thermo Fisher Scientific, Inc.) was applied to measure the concentration of proteins, which were adjusted to a concentration of 6 μg/μl using 1X loading buffer and DEPC water. Then, 5 μl samples was separated by 10% SDS-PAGE gels and then transferred onto polyvinylidene fluoride membranes (EMD Millipore, Billerica, MA, USA). Following blocking of the membranes in 5% nonfat milk in PBST (0.1% Tween-20 in PBS) for 1 h at room temperature, the membranes were probed with the primary antibodies overnight at 4˚C. The membranes were then washed 3 times with PBST and then incubated with horseradish peroxidase (HRP)-conjugated goat anti-mouse (cat. no. sc-516102; 1:2,000) and HRP-rabbit IgG (cat. no. sc-2357; 1:2,000; both Santa Cruz Biotechnology, Inc., Dallas, TX, USA) secondary antibodies at room temperature for 2 h. Then, the membranes were washed 3 times with PBST. The EZ-ECL kit (Biological Industries, Kibbutz Beit Haemek, Israel) was used to visualize the gels, and the gray values were analyzed and counted using ImageJ software (v5.0; Bio-Rad Laboratories, Inc., Hercules, CA, USA). The antibodies used were mouse anti-GAPDH (1:1,000; cat. no. LS-B1625; LifeSpan BioSciences, Inc.), rabbit anti-URG11 (1:1,000; cat. no. ab109232), mouse anti-epithelial cadherin (E-cadherin; 1:1,000; cat. no. ab1416), rabbit anti-Vimentin (1:1,000; cat. no. ab92547) and rabbit anti-α-smooth muscle actin (α-SMA; 1:1,000; cat. no. ab5694), mouse anti-cyclin D1 (1:1,000; cat. no. ab134175) and rabbit anti-MYC proto-oncogene protein (c-Myc; 1:1,000; cat. no. ab32072; all Abcam, Cambridge, MA, USA).

Statistical analysis. The results are presented as the mean ± standard deviation. Statistical software Prism 7 (GraphPad Software, Inc., La Jolla, CA, USA) was used for statistical analysis. Comparisons between two groups were performed using un-paired Student's t-tests, and the comparisons between multiple groups were performed by one-way analysis of variance followed by Dunnett's post hoc test. $P<0.05$ was considered to indicate a statistically significant difference.

Results

URG11 is expressed in cancer cells. The expression levels of URG11 were first investigated in Pca cells lines, including DU145, PC3 and LNCaP cell lines, and in the nontumor prostate epithelial RWPE-1 cell line. The URG11 mRNA levels in human prostate cells were significantly increased compared with that in the epithelial cells (Fig. 1A). Furthermore, western blot analysis was used to determine the URG11 protein level in the Pca cell lines. Similarly, the URG11 protein level exhibited the same pattern of expression as the mRNA level (Fig. 1B and C). Specifically, the LNCaP cells exhibited increased URG11 mRNA and protein expression levels in comparison with DU145 cells and PC3 cells. Therefore, LNCaP cells were used for the subsequent experiments.

Overexpression of URG11 promotes cells viability of cultured LNCaP cells and siURG11 elicits the opposite effect. To additionally explore the function of URG11 in Pca cells, overexpression plasmids and siRNA were applied to overexpress and silence URG11, respectively. Following the transfection of the URG11 plasmids and siURG11 fragments into LNCaP prostate cells, the expression level of URG11 was significantly increased in the URG11 overexpression group but suppressed in the siURG11 group compared with their corresponding control and NC groups at the mRNA (Fig. 2A) and protein levels (Fig. 2B and C). Following confirmation of the efficacy of the overexpression URG11 vector and siURG11 fragments, a CCK-8 assay was then used to detect the effects of URG11 overexpression and silencing on cell viability. As demonstrated in Fig. 2D, the cells in the URG11 overexpression group exhibited increased growth compared with the normal culture and NC groups at 24, 48 and 72 h, while siURG11

Table I. Primers for quantitative polymerase chain reaction.

Genes	Forward (5'-3')	Reverse (5'-3')
URG11	TGAATCAAGGAGTCGCTGGAC	GCATCTCACTGGAACACAAG
E-cadherin	TCGACACCCGATTCAAAGTG	GTCCCAGGCGTAGACCAAGA
Vimentin	TGCCCTTAAAGGAACCAATGAG	AGGCGGCCAATAGTGTCTTG
α-SMA	CTGTTCCAGCCATCCTTCAT	CCGTGATCTCCTTCTGCATT
Cyclin D1	CACACGGACTACAGGGGAGT	CACAGGAGCTGGTGTTCCAT
c-Myc	TCAAGAGGCGAACACACAAC	GGCCTTTTCATTGTTTTCCA
GAPDH	CGCTACAGTCGTTGCCATCA	ACGACGAGGAAGCCATCTTG

URG11, Upregulated 11; E-cadherin, epithelial cadherin; α-SMA, α smooth muscleactin; c-Myc, MYC proto-oncogene protein.

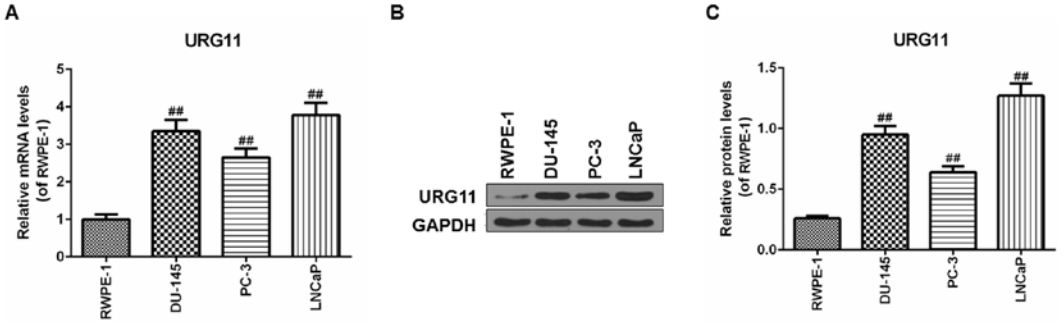

Figure 1. URG11 expression is upregulated in cell lines. (A) The mRNA level of URG11 was determined by reverse transcription quantitative polymerase chain reaction. (B) The protein level of URG11 was measured by western blot analysis. (C) Densitometric analysis data of the western blot analysis. Error bars represent standard deviation. $^{\#\#}$P<0.01 vs. RWPE-1. URG11, von Willebrand factor C and EGF domain-containing protein.

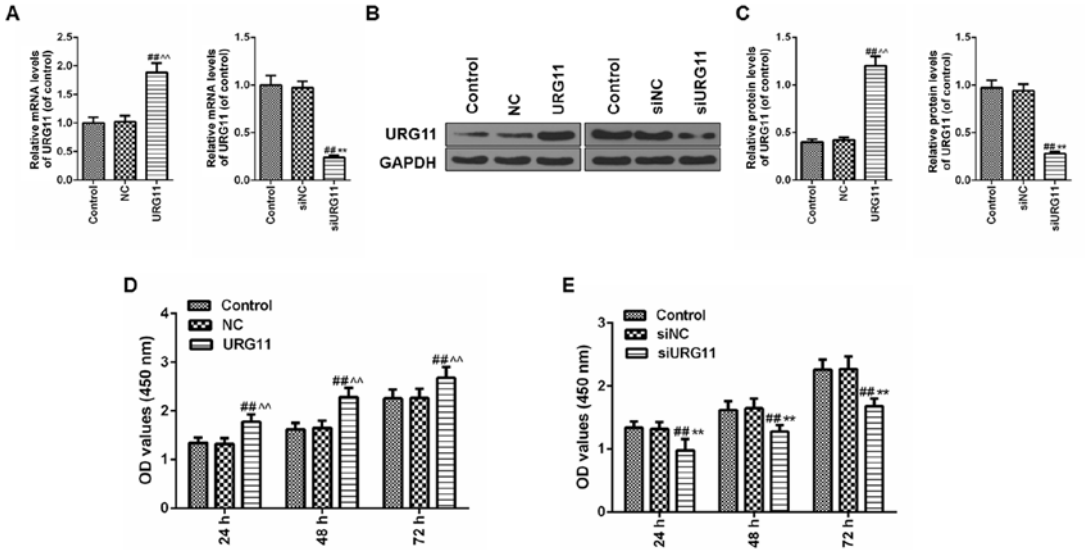

Figure 2. Genetic knockdown of URG11 suppresses viability of prostate cancer cells, while URG11 elicits the opposite effect. (A) Transfection efficiency of URG11 and siURG11 was quantified by reverse transcription quantitative polymerase chain reaction in mRNA levels. (B) Transfection efficiency of URG11 and siURG11 was quantified by western blot analysis at protein levels. (C) Densitometric analysis data of the western blot analysis. (D and E) The viability of cells transfected with (D) UURG11 overexpression plasmids and (E) siURG11 was evaluated using a Cell Counting kit-8 assay. Error bars represent standard deviation. $^{\#\#}$P<0.01 vs. control; $^{\wedge\wedge}$P<0.01 vs. NC; **P<0.01 vs. siNC. URG11, von Willebrand factor C and EGF domain-containing protein; si, small interfering; NC, negative control; OD, optical density.

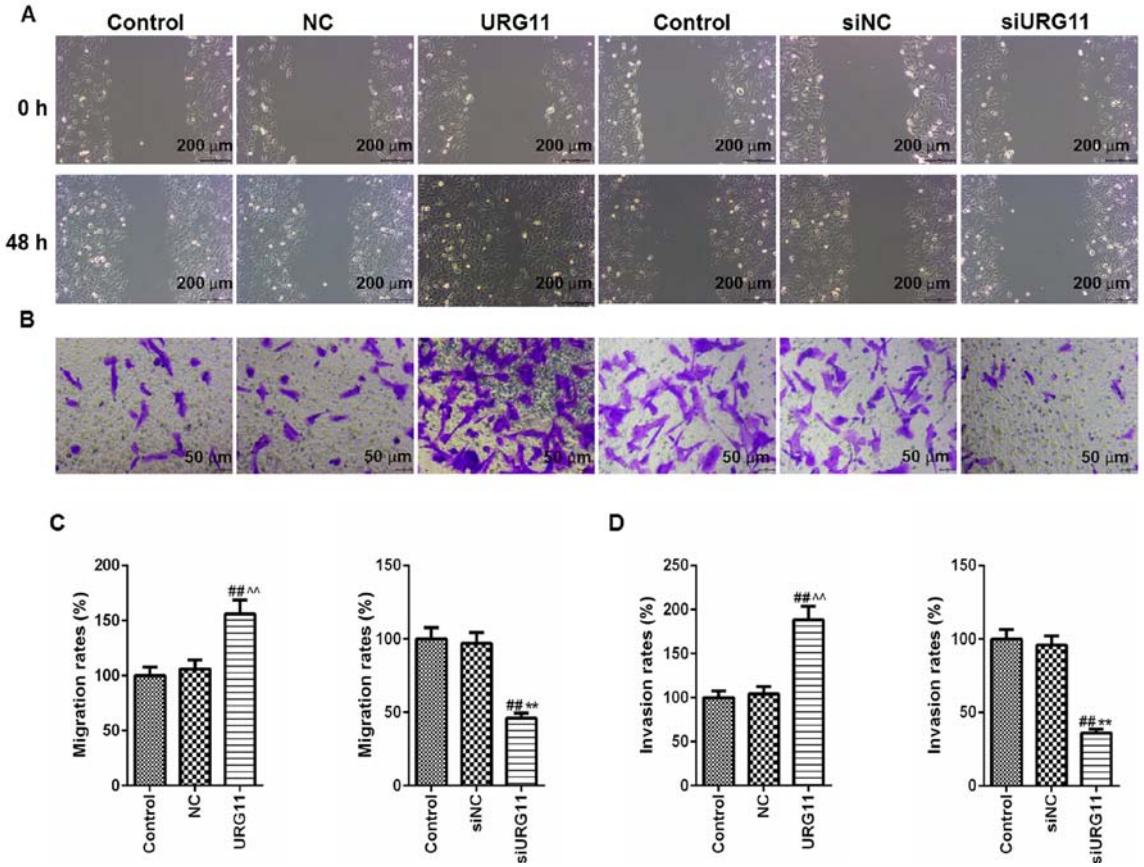

Figure 3. Inhibition of URG11 impairs the migration and invasion of LNCaP cells, while URG11 elicits the opposite effects. (A and B) Representative images from the (A) migration and (B) invasion assays in each group are presented. Magnification, x200. (C and D) Quantified data from the (C) migration and (D) invasion assays. Error bars represent standard deviation. ##P<0.01 vs. control; ^^P<0.01 vs. NC; **P<0.01 vs. siNC. URG11, von Willebrand factor C and EGF domain-containing protein; si, small interfering; NC, negative control.

decreased cell viability compared with the normal culture and NC groups at 24, 48 and 72 h (Fig. 2E).

Overexpression of URG11 promotes migration and invasion of LNCaP cells and siURG11 elicits the opposite effects. The specific role of URG11 in the invasion and migration of Pca cells was then determined. Cell migratory and invasive abilities were determined by wound healing and Transwell assays, respectively. The wounds generated in the cells in the URG11 overexpression group were almost healed at 48 h, at which time the wounds in normal culture and control groups were significantly wider. Treatment with siURG11 exhibited the opposite effects (Fig. 3A). Furthermore, the Transwell invasion assays revealed that the overexpression of URG11 significantly promoted the invasion of LNCaP Pca cells compared with those of in the normal culture and NC control groups, and genetic knockout of URG11 elicited the opposite effects (Fig. 3B). The quantified data from the migration and invasion assays are presented in Fig. 3C and D.

Overexpression of URG11 inhibits apoptosis and induces cell cycle progression, while siURG11 exhibits the opposite effects. To improve understanding of the role of URG11 in Pca metastasis and the underlying mechanism of action, flow cytometry was performed with PI/Annexin V staining for apoptosis and cell cycle analyses. Using flow cytometric analysis with PI/Annexin V staining, overexpression of URG11 was observed to significantly suppress cell apoptosis, compared with that in the normal culture and NC groups (Fig. 4A). Furthermore, overexpression of URG11 significantly decreased the number of cells in G0/G1 phase and increased the number of cells in S phase, compared with that in the normal culture and NC control groups (Fig. 4B). By contrast, siURG11 elicited the opposite effects (Fig. 4A-D).

Overexpression of URG11 inhibits the level of E-cadherin and increases the levels of Vimentin and α-SMA, while siURG11 elicits the opposite effects. Due to the importance of EMT in the development of LNCaP cells, the effect of URG11/siURG11 on EMT markers in LNCaP cells was assessed. The mRNA and protein levels of EMT markers were examined by RT-qPCR and western blot analysis, respectively. As indicated in Fig. 5A, overexpression URG11 treatment significantly decreased E-cadherin mRNA levels and increased vimentin and α-SMA mRNA levels compared with the controls (Fig. 5A). Furthermore, western blot analysis was used to determine the protein levels of those EMT markers, and the results demonstrated that the effects of URG11 on protein levels of E-cadherin, vimentin and α-SMA were in accordance with mRNA levels (Fig. 5B and C). However, siURG11 elicited the opposite effects (Fig. 5D-F).

URG11 significantly increases the expression of cyclin D1 and c-Myc in LNCaP cells, while siURG11 inhibits the levels

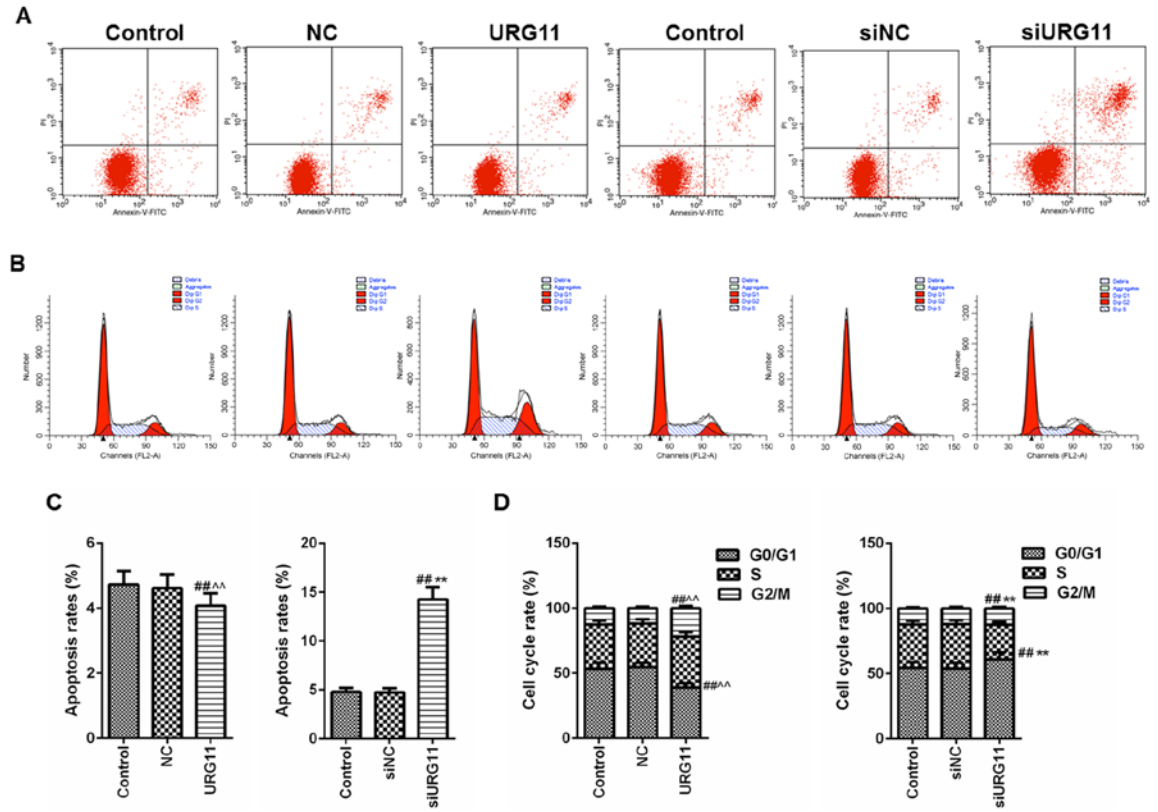

Figure 4. Inhibition of URG11 induces cell cycle arrest and apoptosis of LNCaP cells. (A and B) Flow cytometry was performed to measure (A) levels of apoptosis and (B) cell cycle. (C and D) Quantification of (C) the apoptosis and (D) cell cycle analyses data. Error bars represent standard deviation. ##P<0.01 vs. control; ^^P<0.01 vs. NC; **P<0.01 vs. siNC. URG11, von Willebrand factor C and EGF domain-containing protein; si, small interfering; NC, negative control; PI, propidium iodide; FITC, fluorescein isothiocyanate.

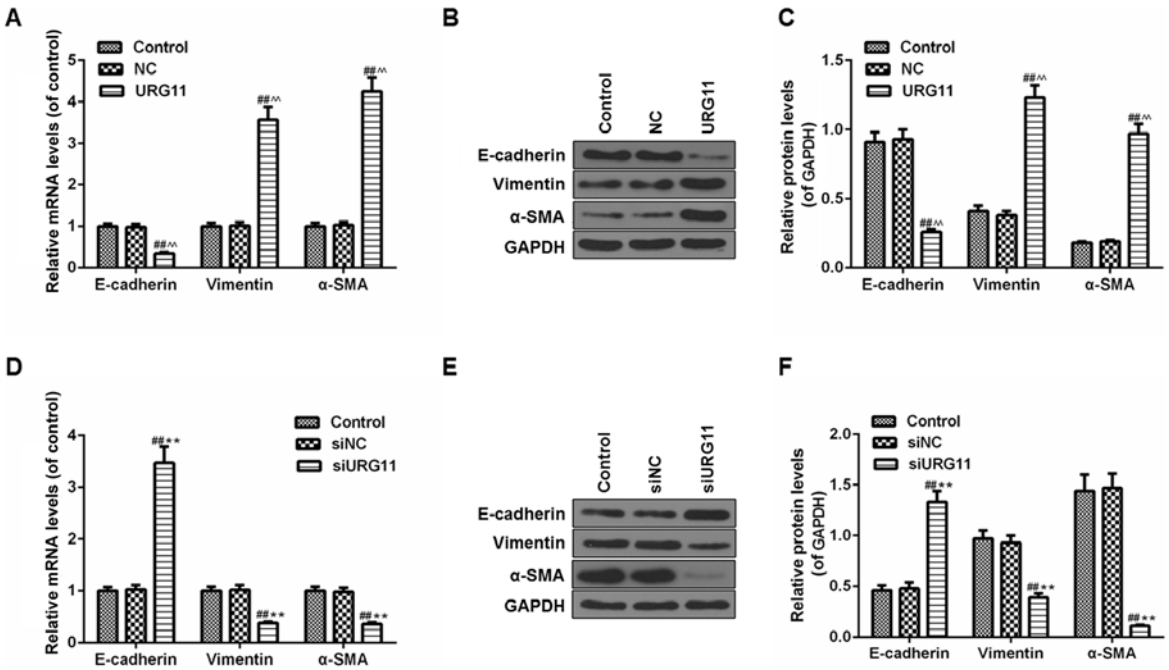

Figure 5. Effects of URG11 and siURG11 on EMT in LNCaP cells. (A) The mRNA levels of EMT markers (E-cadherin, vimentin and α-SMA) in URG11-overexpressing cells were determined by RT-qPCR. (B) The protein levels of EMT markers (E-cadherin, vimentin and α-SMA) in URG11-overexpressing cells were quantified by western blot analysis. (C) Densitometric analysis of the EMT protein levels in URG11-overexpressing cells, normalized to GAPDH. (D) The mRNA levels of EMT markers (E-cadherin, vimentin and α-SMA) in URG11-knockout cells were determined by RT-qPCR. (E) The protein levels of EMT markers (E-cadherin, vimentin and α-SMA) in URG11-knockout cells were quantified by western blot analysis. (F) Densitometric analysis of the EMT protein levels in URG11-knockout cells, normalized to GAPDH. Error bars represent standard deviation. ##P<0.01 vs. control; ^^P<0.01 vs. NC; **P<0.01 vs. siNC. si, small interfering; URG11, von Willebrand factor C and EGF domain-containing protein; EMT, epithelial-mesenchymal transition; RT-qPCR, reverse transcription quantitative polymerase chain reaction; E-cadherin, epithelial cadherin; α-SMA, α smooth muscle actin; NC, negative control.

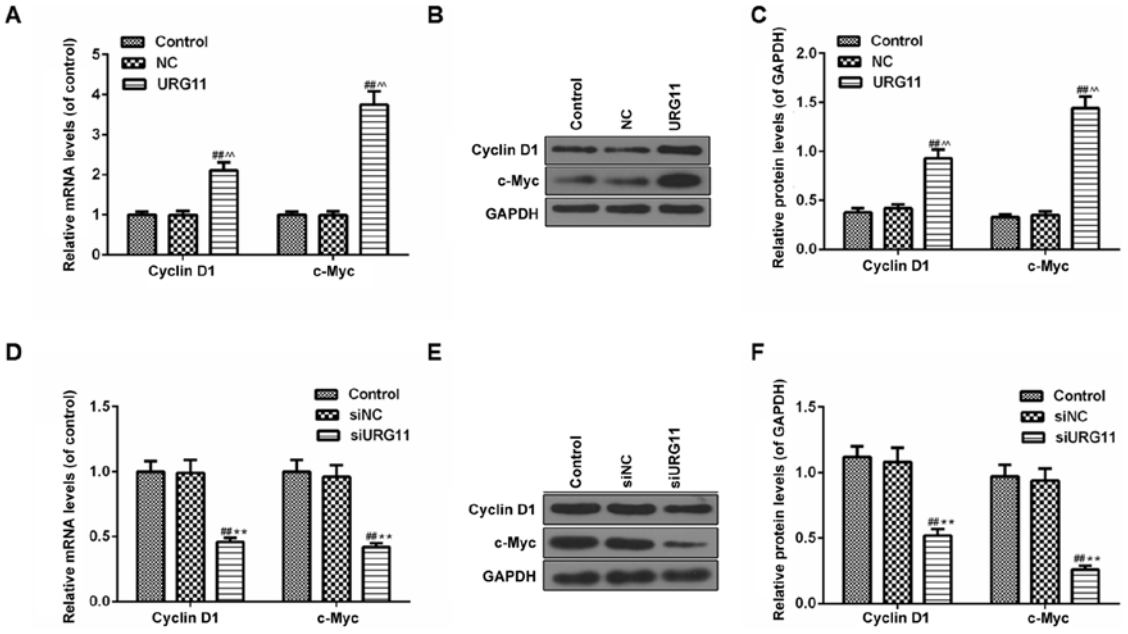

Figure 6. URG11 significantly increases the expression of cyclin D1 and c-Myc in LNCaP cells, while siURG11 elicits the opposite effect. (A) The mRNA levels of cyclin D1 and c-Myc in URG11-overexpressing cells were determined by RT-qPCR. (B) The protein levels of cyclin D1 and c-Myc in URG11-overexpressing cells were quantified by western blot analysis. (C) Densitometric analysis of the cyclin D1 and c-Myc protein levels in URG11-overexpressing cells, normalized to GAPDH. (D) The mRNA levels of cyclin D1 and c-Myc in URG11-knockout cells were determined by RT-qPCR. (E) The protein levels of cyclin D1 and c-Myc in URG11-knockout cells were quantified by western blot analysis. (F) Densitometric analysis of the cyclin D1 and c-Myc protein levels in URG11-knockout cells, normalized to GAPDH. Error bars represent standard deviation. $^{\#\#}$P<0.01 vs. control, $^{\wedge\wedge}$P<0.01 vs. NC, **P<0.01 vs. siNC. URG11, von Willebrand factor C and EGF domain-containing protein; c-Myc, MYC proto-oncogene protein; si, small interfering; RT-qPCR, reverse transcription quantitative polymerase chain reaction; NC, negative control.

of cyclin D1 and c-Myc. As the overexpression of URG11 and siURG11 significantly affected proliferation and cell cycle arrest in human LNCaP cells, western blot analysis was performed to examine the protein expression levels of cyclin D1 and c-Myc, which are involved in the regulation of cell proliferation and the cell cycle. It was identified that the transfection of LNCaP cells with URG11 overexpression plasmid vectors significantly promoted the expression of cyclin D1 and c-Myc at the mRNA (Fig. 6A) and protein levels (Fig. 6B and C). However, gene knockdown of URG11 markedly inhibited the levels of cyclin D1 and c-Myc at the mRNA (Fig. 6D) and protein levels (Fig. 6E and F).

URG11 promotes cell viability, migration and invasion, which is reversed by FH535. Due to the importance of Wnt/β-catenin signal pathway in URG11-induced cell viability, migration and invasion in LNCaP cells, the cells were treated with URG11 overexpression plasmids and the Wnt/β-catenin inhibitor FH535 (20 μM), together and individually. Then, the cell viability, migration and invasion were respectively determined by CCK-8, wound healing and Transwell assays. With these functional experiments, it was identified that FH535 treatment significantly inhibited the plasmid vector URG11 transfection-induced effects on cell viability (Fig. 7A), migration (Fig. 7B and D) and invasion (Fig. 7C and E). The images of migration and invasion were presented in Fig. 7D and E, respectively.

URG11 knockdown suppresses cell viability, migration and invasion, which is reversed by LiCl. In order to additionally validate the role of the Wnt/β-catenin signaling pathway in LNCaP cells proliferation, the cells were treated with siURG11 and the Wnt/β-catenin agonist LiCl (20 μM), together and individually. CCK-8, wound healing and Transwell assays were also conducted to determine the effects on cell viability, migration and invasion, respectively. Notably, it was identified that that the cell viability (Fig. 8A), migration (Fig. 8B) and invasion (Fig. 8C) were increased in the siURG11+ LiCl group compared with those in the siURG11 group. The images of migration and invasion were presented in Fig. 8D and E.

Discussion

Pca is the most common malignant tumor of the male genitourinary system, and exhibited the fifth highest incidence rate in 2008 worldwide (24). Numerous studies have identified various agents that are able to treat cancer cells; however, the majority of clinical trials have failed to provide promising treatment options due to their inefficiency or unexpected side effects (25,26). Therefore, studies investigating novel molecules that may serve key roles in the development of Pca will assist in developing novel therapeutic methods and targets, which may be crucial for the improvement of the treatment and prognoses of patients with Pca.

As an effector of hepatitis B virus X protein, URG11 is upregulated in various types of human cancer, including hepatocellular carcinoma (8), and gastric (9) and colon cancer (12). In 2018, Pan *et al* (12) identified that URG11 was significantly upregulated in Pca. These studies indicated that URG11 served an important role in the development of these types of cancer. However, the underlying mechanisms of the URG11 gene in Pca cells remain unknown.

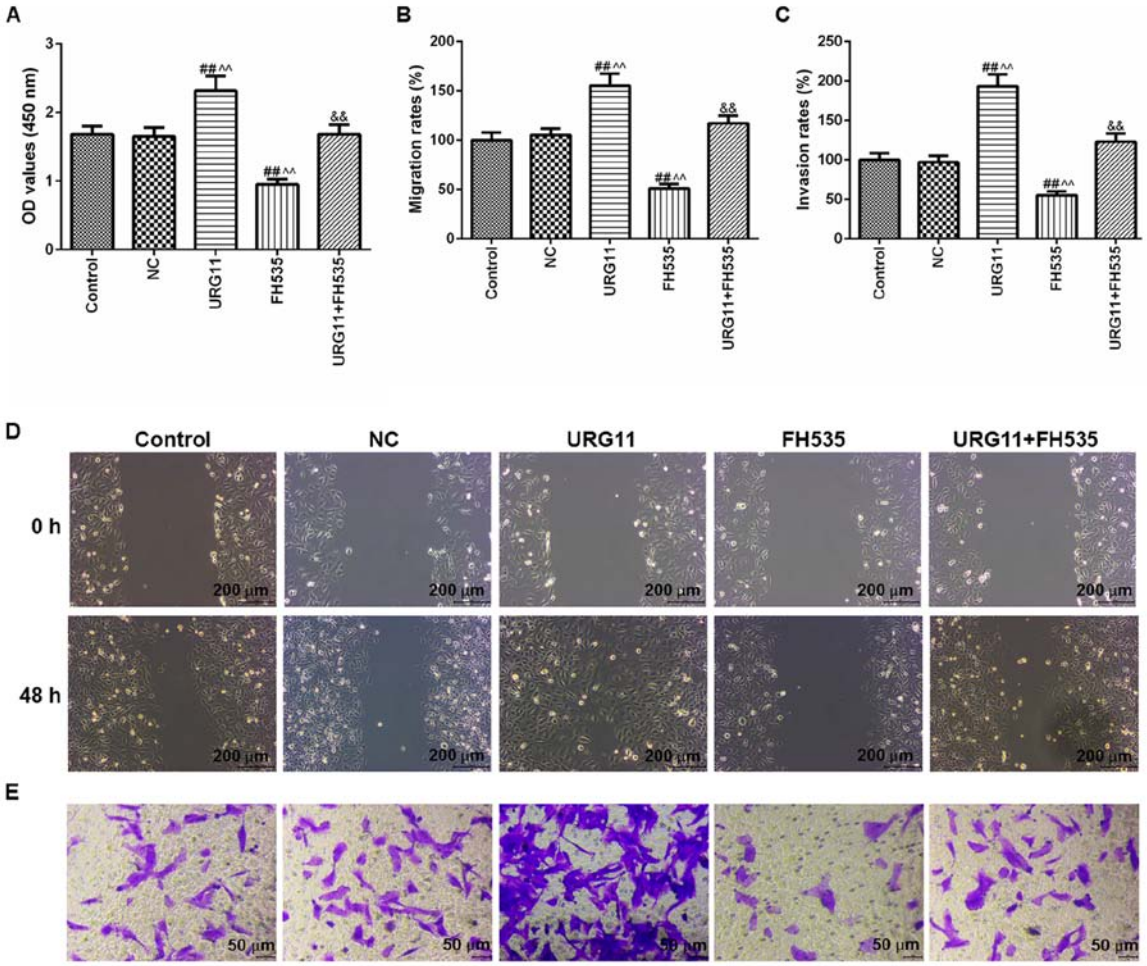

Figure 7. URG11 overexpression promotes cell viability, migration and invasion, which is reversed by FH535. (A) The viability of cell was examined using a Cell Counting kit-8 assay. (B) Migration was measured using a wound heading assay. (C) Invasion was evaluated using a Transwell assay. (D and E) Representative images from the (D) migration and (E) invasion assays in each group. Magnification, x200. Error bars represent standard deviation. $^{\#\#}$P<0.01 vs. control; $^{\wedge\wedge}$P<0.01 vs. NC; $^{\&\&}$P<0.01 vs. FH535. URG11, von Willebrand factor C and EGF domain-containing protein; NC, negative control; OD, optical density.

According to a previous study, Peng *et al* (10) identified that URG11 promoted pancreatic cancer invasion through EMT, leading to poor prognosis. Fan *et al* (6) demonstrated that the inhibition of URG11 on hepatocellular carcinoma cells inhibited cell proliferation by downregulating G1-S phase-associated proteins, and induced apoptosis by downregulating B cell lymphoma 2. Gene knockdown by URG11 inhibited proliferation of pancreatic cancer cells and suppressed invasion (10). Consistent with previous studies, the data from the present study indicated that URG11 was significantly upregulated in Pca cell lines, and that the overexpression of URG11 promoted cell viability, migration and invasion, and inhibited apoptosis and cell cycle arrest, whereas inhibition of URG11 expression by interference RNA suppressed cell viability, metastasis and invasion, and induced apoptosis and cell cycle arrest. These data suggested that URG11 may be involved in the development of Pca, as demonstrated by its effects in LNCaP cells.

EMT is widely regarded as one of the important factors that contribute to tumor invasion and metastasis (27). Downregulation of epithelial tissue markers and upregulation of mesenchymal tissue markers are important molecular events in the development of EMT (28). Silencing URG11 expression inhibited EMT by altering E-cadherin, neural cadherin and vimentin levels in prostatic hyperplasia cells (29). Overexpression of URG11 promoted EMT accompanied by a downregulation of the epithelial marker E-cadherin and upregulation of the mesenchymal markers vimentin and α-SMA in a human proximal tubule cell line (30). The present study identified that overexpression of URG11 attenuated the expression of E-cadherin and increased the expression levels of vimentin and α-SMA in LNCaP cells, while URG11 knockdown by siRNA effectively reversed this effect on the EMT-associated proteins in the LNCaP cells. These data demonstrated that URG11 accelerated the progression of Pca by activating EMT. Therefore, targeting EMT may be a promising treatment strategy for the management of Pca.

Wnt/β-catenin signaling pathway is an important mechanism of action in various tumorigenesis and development processes (31). The Wnt/β-catenin pathway controls the expression of a number of downstream target genes including cyclin D1 and c-Myc, thereby promoting tumorigenesis (32,33). At present, β-catenin mutations or dysregulation have been identified in various types of tumors including colorectal (34), renal (35), gastric (36) and liver cancer (37), and they participate in tumorigenesis and malignant progression.

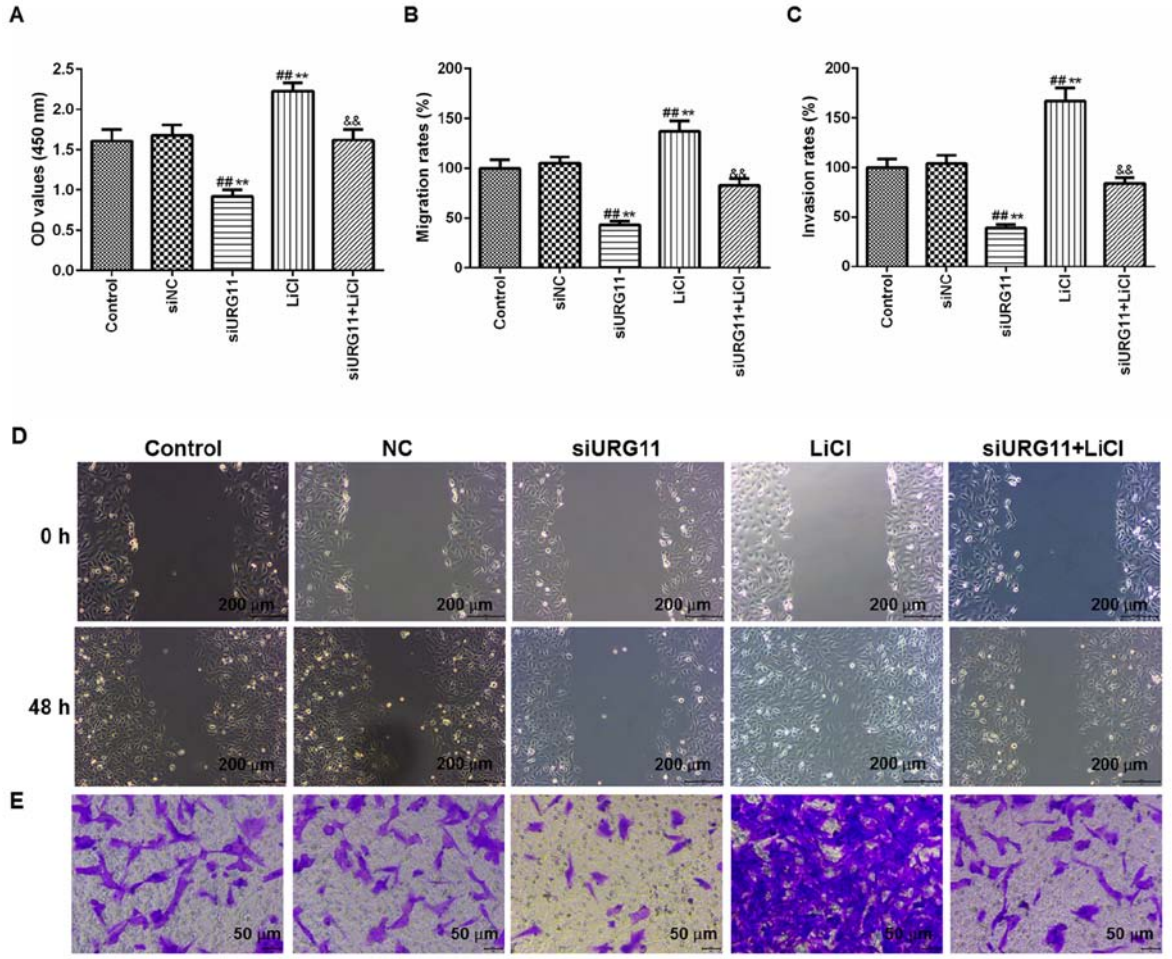

Figure 8. Knockdown of URG11 suppresses cell viability, migration and invasion, which is reversed by LiCl. (A) The viability of cell was measured using a Cell Counting kit-8. (B) Migration was detected by a wound heading assay. (C) Invasion was determined using a Transwell assay. (D and E) Representative images from the (D) migration and (E) invasion assays in each group, respectively. Magnification, x200. Error bars represent standard deviation. $^{\#\#}$P<0.01 vs. control; **P<0.01 vs. siNC; $^{\&\&}$P<0.01 vs. LiCl. URG11, von Willebrand factor C and EGF domain-containing protein; si, small interfering; NC, negative control; OD, optical density.

A previous study suggested that knockdown of URG11 inhibited β-catenin expression in non-small cell lung cancer cells (11). Accumulating studies have indicated that aberrant activation of Wnt/β-catenin pathway is implicated in Pca tumorigenesis (38-40). In the present study, it was identified that the mRNA and protein levels of cyclin D1 and c-Myc were increased following URG11 overexpression. However, knockdown of UGR11 effectively inhibited the expression of cyclin D1 and c-Myc. LNCaP cells were treated with URG11 overexpression plasmids and Wnt/β-catenin pathway inhibitor FH535, and with siURG11 and Wnt/β-catenin pathway agonist LiCl; the results indicated that cell viability, migration and invasion may be reversed in comparison with the URG11 and siURG11 group, respectively. These results suggested that the regulation of URG11 in Pca may be associated with the Wnt/β-catenin signaling pathway. However, certain aspects of the present study require additional investigation, including the role of URG11 in Pca *in vivo*.

In conclusion, the present study provided evidence that URG11 was positively associated with Pca tumorigenesis and metastasis, and that the overexpression of URG11 promoted proliferation, migration and invasion, and was involved in the Wnt/β-catenin signaling pathway in Pca cells, while treatment with siURG11 elicited the opposite effects. Taken together, these data suggested that URG11 may serve an oncogene role in Pca, and that URG11 may be involved in the early development and progression of Pca. URG11 may be a potential novel clinical target for Pca.

Acknowledgements

Not applicable.

Funding

No funding was received.

Availability of data and materials

The analyzed data sets generated during the present study are available from the corresponding author on reasonable request.

Authors' contributions

CS made substantial contributions to the conception and design of the study. GZ and ML were responsible for data acquisition,

data analysis and interpretation. SC and HQ drafted the article and critically revised it for important intellectual content. All authors provided final approval of the version to publish. DL and CS agree to be accountable for all aspects of the work in ensuring that questions related to the accuracy or integrity of the work are appropriately investigated and resolved.

Ethics approval and consent to participate

Not applicable.

Patient consent for publication

Not applicable.

Competing interests

The authors declare that they have no competing interests.

References

1. Jemal A, Bray F, Center MM, Ferlay J, Ward E and Forman D: Global cancer statistics. CA Cancer J Clin 61: 69-90, 2011.
2. VanderWalde A and Hurria A: Aging and osteoporosis in breast and prostate cancer. CA Cancer J Clin 61: 139-156, 2011.
3. Nelson BA, Shappell SB, Chang SS, Wells N, Farnham SB, Smith JA Jr and Cookson MS: Tumour volume is an independent predictor of prostate-specific antigen recurrence in patients undergoing radical prostatectomy for clinically localized prostate cancer. BJU Int 97: 1169-1172, 2006.
4. Zhang HF, Wang HL, Xu N, Li SW, Ji GY, Li XM, Pan YZ, Zhang L, Zhao XJ and Gao HW: Mass screening of 12,027 elderly men for prostate carcinoma by measuring serum prostate specific antigen. Chin Med J (Engl) 117: 67-70, 2004.
5. Jin Y, Chen Y, Jiang Y and Xu M: Proteome analysis of the silkworm (*Bombyx mori*. L) colleterial gland during different development stages. Arch Insect Biochem Physiol 61: 42-50, 2006.
6. Fan R, Li X, Du W, Zou X, Du R, Zhao L, Luo G, Mo P, Xia L, Pan Y, *et al*: Adenoviral-mediated RNA interference targeting URG11 inhibits growth of human hepatocellular carcinoma. Int J Cancer 128: 2980-2993, 2011.
7. Lian Z, Liu J, Li L, Li X, Tufan NL, Clayton M, Wu MC, Wang HY, Arbuthnot P, Kew M, et al: Upregulated expression of a unique gene by hepatitis B x antigen promotes hepatocellular growth and tumorigenesis. Neoplasia 5: 229-244, 2003.
8. Xie H and Liu J: Increased expression URG11 in hepatocellular carcinoma tissues promotes the growth of hepatocellular carcinoma cells. Xi bao yu fen zi mian yi xue za zhi 31: 1523-1527, 2015 (In Chinese).
9. Du R, Xia L, Sun S, Lian Z, Zou X, Gao J, Xie H, Fan R, Song J, Li X, et al: URG11 promotes gastric cancer growth and invasion by activation of beta-catenin signalling pathway. J Cell Mol Med 14: 621-635, 2010.
10. Peng W, Zhang J and Liu J: URG11 predicts poor prognosis of pancreatic cancer by enhancing epithelial-mesenchymal transition-driven invasion. Med Oncol 31: 64, 2014.
11. Liu ZL, Wu J, Wang LX, Yang JF, Xiao GM, Sun HP and Chen YJ: Knockdown of Upregulated Gene 11 (URG11) Inhibits Proliferation, Invasion, and β-Catenin Expression in Non-Small Cell Lung Cancer Cells. Oncol Res 24: 197-204, 2016.
12. Pan B, Ye Y, Liu H, Zhen J, Zhou H, Li Y, Qu L, Wu Y, Zeng C and Zhong W: URG11 regulates prostate cancer cell proliferation, migration, and invasion. BioMed Res Int 2018: 4060728, 2018.
13. Chen Y, Tan W and Wang C: Tumor-associated macrophage-derived cytokines enhance cancer stem-like characteristics through epithelial-mesenchymal transition. OncoTargets Ther 11: 3817-3826, 2018.
14. Yan L, Xu F and Dai CL: Relationship between epithelial-to-mesenchymal transition and the inflammatory microenvironment of hepatocellular carcinoma. J Exp Clin Cancer Res 37: 203, 2018.
15. Brennen WN and Isaacs JT: Mesenchymal stem cells and the embryonic reawakening theory of BPH. Nat Rev Urol 15: 703-715, 2018.
16. Usova EV, Kopantseva MR, Egorov VI, Kopantzev EP and Sverdlov ED: SNAI1 and SNAI2 - transcriptional master-regulators of epithelial-mesenchimal transition. Patol Fiziol Eksp Ter 59: 76-87, 2015 (In Russian).
17. Sung CO, Park CK and Kim SH: Classification of epithelial-mesenchymal transition phenotypes in esophageal squamous cell carcinoma is strongly associated with patient prognosis. Modern pathology: An official journal of the United States and Canadian Academy of Pathology. Inc 24: 1060-1068, 2011.
18. Inoue T, Umezawa A, Takenaka T, Suzuki H and Okada H: The contribution of epithelial-mesenchymal transition to renal fibrosis differs among kidney disease models. Kidney Int 87: 233-238, 2015.
19. Lim SH, Becker TM, Chua W, Ng WL, de Souza P and Spring KJ: Circulating tumour cells and the epithelial mesenchymal transition in colorectal cancer. J Clin Pathol 67: 848-853, 2014.
20. Giles RH, van Es JH and Clevers H: Caught up in a Wnt storm: Wnt signaling in cancer. Biochim Biophys Acta 1653: 1-24, 2003.
21. Rabbani SA, Arakelian A and Farookhi R: LRP5 knockdown: Effect on prostate cancer invasion growth and skeletal metastasis in vitro and in vivo. Cancer Med 2: 625-635, 2013.
22. Dai J, Hall CL, Escara-Wilke J, Mizokami A, Keller JM and Keller ET: Prostate cancer induces bone metastasis through Wnt-induced bone morphogenetic protein-dependent and independent mechanisms. Cancer Res 68: 5785-5794, 2008.
23. Livak KJ and Schmittgen TD: Analysis of relative gene expression data using real-time quantitative PCR and the 2(-Delta Delta C(T)) method. Methods 25: 402-408, 2001.
24. Ferlay J, Shin HR, Bray F, Forman D, Mathers C and Parkin DM: Estimates of worldwide burden of cancer in 2008: Globocan 2008. Int J Cancer 127: 2893-2917, 2010.
25. Chang L, Graham PH, Hao J, Bucci J, Cozzi PJ, Kearsley JH and Li Y: Emerging roles of radioresistance in prostate cancer metastasis and radiation therapy. Cancer Metastasis Rev 33: 469-496, 2014.
26. Alberti C: Prostate cancer: Radioresistance molecular target-related markers and foreseeable modalities of radiosensitization. Eur Rev Med Pharmacol Sci 18: 2275-2282, 2014.
27. Singh A and Settleman J: EMT, cancer stem cells and drug resistance: An emerging axis of evil in the war on cancer. Oncogene 29: 4741-4751, 2010.
28. Bronsert P, Enderle-Ammour K, Bader M, Timme S, Kuehs M, Csanadi A, Kayser G, Kohler I, Bausch D, Hoeppner J, *et al*: Cancer cell invasion and EMT marker expression: A three-dimensional study of the human cancer-host interface. J Pathol 234: 410-422, 2014.
29. Zhang G, Zhu F, Han G, Li Z, Yu Q, Li Z and Li J: Silencing of URG11 expression inhibits the proliferation and epithelial mesenchymal transition in benign prostatic hyperplasia cells via the RhoA/ROCK1 pathway. Mol Med Rep 18: 391-398, 2018.
30. Du R, Huang C, Bi Q, Zhai Y, Xia L, Liu J, Sun S and Fan D: URG11 mediates hypoxia-induced epithelial-to-mesenchymal transition by modulation of E-cadherin and β-catenin. Biochem Biophys Res Commun 391: 135-141, 2010.
31. Gupta A, Verma A, Mishra AK, Wadhwa G, Sharma SK and Jain CK: The Wnt pathway: Emerging anticancer strategies. Recent Pat Endocr Metab Immune Drug Discov 7: 138-147, 2013.
32. Vallée A, Lecarpentier Y, Guillevin R and Vallée JN: Thermodynamics in gliomas: Interactions between the canonical WNT/beta-catenin pathway and PPAR gamma. Front Physiol 8: 352, 2017.
33. Tang X, Wang Y, Fan Z, Ji G, Wang M, Lin J, Huang S and Meltzer SJ: Klotho: A tumor suppressor and modulator of the Wnt/β-catenin pathway in human hepatocellular carcinoma. Lab Invest 96: 197-205, 2016.
34. Pandurangan AK, Divya T, Kumar K, Dineshbabu V, Velavan B and Sudhandiran G: Colorectal carcinogenesis: Insights into the cell death and signal transduction pathways: A review. World J Gastrointest Oncol 10: 244-259, 2018.
35. Li YL, Jin YF, Liu XX and Li HJ: A comprehensive analysis of Wnt/β-catenin signaling pathway-related genes and crosstalk pathways in the treatment of As2O3 in renal cancer. Ren Fail 40: 331-339, 2018.
36. Yang XZ, Cheng TT, He QJ, Lei ZY, Chi J, Tang Z, Liao QX, Zhang H, Zeng LS and Cui SZ: LINC01133 as ceRNA inhibits gastric cancer progression by sponging miR-106a-3p to regulate APC expression and the Wnt/β-catenin pathway. Mol Cancer 17: 126, 2018.

37. Adebayo Michael AO, Ko S, Tao J, Moghe A, Yang H, Xu M, Russell JO, Pradhan-Sundd T, Liu S, Singh S, *et al*: Inhibiting glutamine-dependent mTORC1 activation ameliorates Liver cancers driven by β-catenin mutations. Cell Metab: Jan 28, 2019 (Epub ahead of print).
38. Ren W, Wang D, Li C, Shu T, Zhang W and Fu X: Capn4 expression is modulated by microRNA-520b and exerts an oncogenic role in prostate cancer cells by promoting Wnt/beta-catenin signaling. Biomed Pharmacother 108: 467-475, 2018.
39. Zhang Z, Cheng L, Li J, Farah E, Atallah NM, Pascuzzi PE, Gupta S and Liu X: Inhibition of the Wnt/β-catenin pathway overcomes resistance to enzalutamide in castration-resistant prostate cancer. Cancer Res 78: 3147-3162, 2018.
40. Sha J, Han Q, Chi C, Zhu Y, Pan J, Dong B, Huang Y, Xia W and Xue W: PRKAR2B promotes prostate cancer metastasis by activating Wnt/β-catenin and inducing epithelial-mesenchymal transition. J Cell Biochem 119: 7319-7327, 2018.